



Enhanced stress wave analysis of scaled monopiles in glacial till at Cowden

Sarah C. Martinⁱ⁾, Róisín M. Buckleyⁱⁱ⁾, Ross A. McAdamⁱⁱⁱ⁾ and Byron W. Byrne^{iv)}

i) DPhil Student, Department of Engineering Science, University of Oxford, Parks Road, Oxford OX1 3PJ, United Kingdom.

ii) Lecturer, School of Engineering, University of Glasgow, Rankine Building, Oakfield Avenue, Glasgow G12 8QQ, United Kingdom.

iii) Associate Professor, Department of Engineering Science, University of Oxford, Parks Road, Oxford OX1 3PJ, United Kingdom.

iv) Professor, Department of Engineering Science, University of Oxford, Parks Road, Oxford OX1 3PJ, United Kingdom.

ABSTRACT

Conventional stress wave analysis for pile driving involves a subjective signal matching process using pile driving analyser (PDA) measurements. The PICASO (Pile Cyclic AnalySis: Oxford and Ørsted) research project provided an opportunity to collect high frequency strain measurements using optical fibre Bragg grating (FBG) sensors over the embedded length of the pile, in addition to conventional PDA data. This paper reports the application of a novel hybrid approach incorporating FBG data into the signal matching process, as developed by Buckley et al. (2020a), to an over-consolidated glacial till site in Cowden, Hull, UK. The additional information on stress wave propagation, obtained through FBG measurements, provides insights into the development of soil resistance to driving (SRD) in stiff clays. The results obtained using the new framework are compared to the resistance predicted using a widely-adopted empirical method.

Keywords: piling, stress wave analysis, field testing, glacial till

1 INTRODUCTION

Large diameter driven tubular steel piles are routinely used to support major offshore wind and near-shore structures. Piles monitored dynamically during driving are fitted with accelerometers and strain gauges near the pile head and above ground level, to measure the strain and acceleration response for each hammer blow. Signal matching can be used to determine the axial pile capacity, traditionally by modelling of the force and velocity traces at the pile head. Driveability analysis, the inverse of signal matching, aims to assess the hammer required to install a pile of a given geometry to the required depth, without imposing excessive driving stresses. Driveability predictions require information on the soil resistance to driving (SRD) along the shaft and at the pile base. Empirical formulations are typically used to link SRD to in-situ measurements, such as the cone penetration test (CPT). In practice, the Alm and Hamre (2001) method, calibrated for long slender piles used in the oil and gas industry, is widely adopted to estimate SRD for driveability analysis.

The PICASO (Pile Cyclic AnalySis: Oxford and Ørsted) research project aims to investigate the response of monopile foundations to lateral cyclic loading. A total of 24 tubular steel piles (11 test piles and 13 reaction piles) were installed in saturated predominantly over-consolidated glacial clay interbedded with thin layers of

silty sand at a site in Cowden, UK (Buckley et al., 2020b). The test pile diameters range from 1.22m to 2.5m with L/D ratios of 3 and diameter-to-wall thickness ratios (D/t) of 69 to 87. The test piles were instrumented with strain and temperature optical fibre Bragg grating (FBG) sensors capable of being logged at a frequency of 5kHz during pile driving. A subset of the test piles was also monitored using conventional pile driving analyser (PDA) sensors, logging at 40kHz during installation. Monotonic and cyclic lateral loading of the test piles has subsequently been completed.

The use of optical FBG sensors to measure strain during pile installation offers potential improvements to the calculation of SRD from the numerical solution of the one-dimensional wave equation. Buckley et al. (2020a) presented a framework that further constrained the signal matching problem by combining conventional pile driving analyser (PDA) with below ground FBG measurements in a hybrid signal matching approach. The PICASO project offered an opportunity to extend the proposed method to a test site involving a different soil profile and the driving of piles with low diameter to wall thickness ratios.

2 SITE DESCRIPTION

The PICASO project involves installation and testing of open-ended steel tubular piles at sites representative

of conditions encountered in the North Sea; (i) an overconsolidated clay site, (ii) a medium dense to dense sand site. This paper relates only to the clay site which was located at Cowden, Hull, United Kingdom (UK Grid Ref: TA 23494 40322). The site is approximately 1km south-west, and in the same geological unit (Devensian Till (BGS, 2015)), as historic PISA and BRE sites used for geotechnical testing. These sites have been characterised by Zdravkovic et al. (2019) and Powell and Butcher (2003) respectively.

A geotechnical investigation was conducted at the PICASO site, including 23 cone penetration tests (CPTs) with pore water pressure measurement and six Geobore-S boreholes (BHs). Low to intermediate plasticity glacial till was encountered from surface to the extent of investigation (20m) with the exception of approximately 1m thick sandy silt layers encountered at variable depths.

Figure 1 shows the range and average of CPT corrected cone resistance, q_t , with RL. Typically q_t is observed to be in the range of 2 to 5MPa with an increase to 6MPa near the base of the large diameter piles, due to the presence of the sandy silt layer. Figure 1 also shows the results of 3 seismic CPTs (SCPTs) with a linear fit of their average taken as the shear modulus, G_{max} , profile for the site. The shear modulus is seen to increase from 100 to 160MPa over the depth range of the large diameter piles.

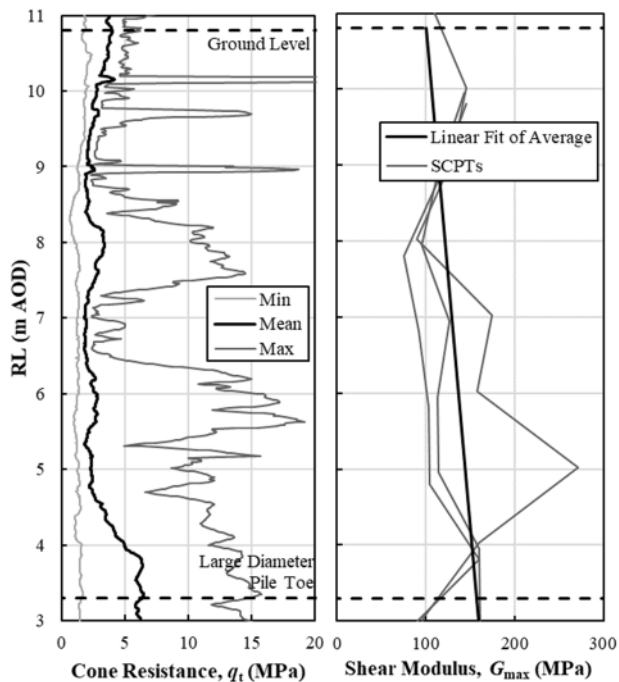


Fig. 1. CPT cone resistance, q_t and shear modulus, G_{max} .

3 TEST PILE AND INSTRUMENT DETAILS

3.1 Pile details

A total of 10 instrumented open-ended tubular steel piles were installed at the site using impact driving, and an additional 1 using vibratory methods between July and August 2020. Pile geometries are illustrated in

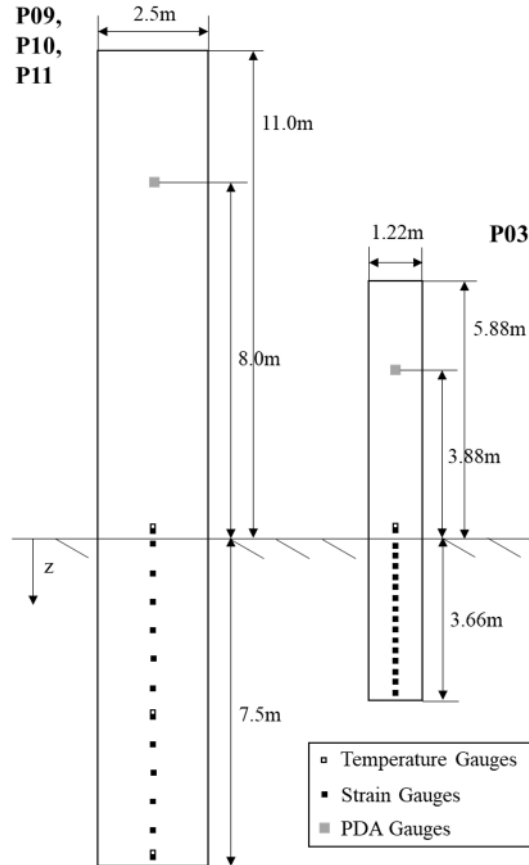


Fig. 2. Pile geometry and layout of FBG and PDA gauges.

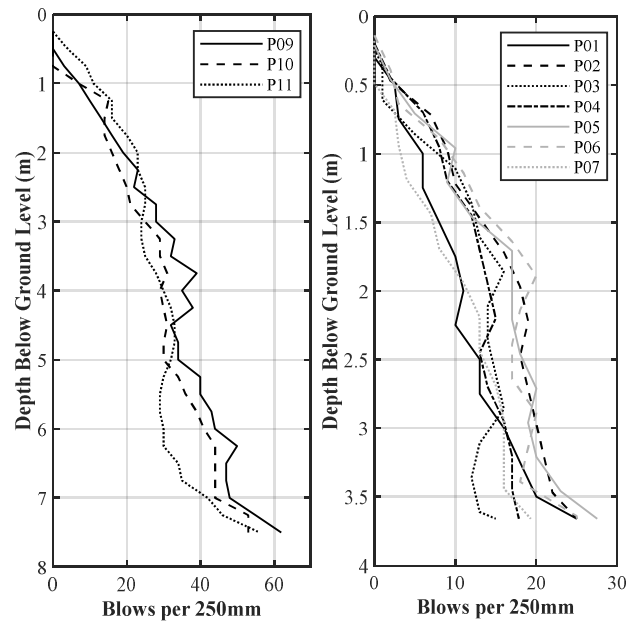


Fig. 3. Blow count profile for large and small diameter piles.

Figure 2. Three instrumented piles were of diameter $D=2.5\text{m}$, wall thickness $t=36\text{mm}$, steel grade S355, and installed using a BSP Hydraulic Hammer CG300 – these are referred to as large diameter piles. Eight instrumented piles were of diameter $D=1.22\text{m}$, one of which had wall thickness $t=16\text{mm}$ and the remainder $t=14\text{mm}$, all of steel grade S420 – these are referred to

as small diameter piles. One small diameter pile was installed using a Liebherr LRB125 Piling Rig with 1100H Vibratory Hammer, while all other small diameter piles were installed using a BSP Hydraulic Hammer CX110/3. All test piles were installed to a depth of 3 times pile diameter with a finished stick-up height above the ground of 4 times pile diameter plus 1m to facilitate later lateral loading. The blow count profiles for all instrumented driven piles are shown in Figure 3. This shows local variation across the site, with below average resistance experienced early in driving for P01 and P07, and near the end of driving for P03 and P11.

3.2 Instrumentation

PDA strain gauges and accelerometers were attached to four piles, logging at a frequency of 40kHz using proprietary software. This allows calculation of force and velocity at the pile top for each hammer blow. For small diameter pile P03, PDA gauges were located 2m below the pile top and for large diameter piles P09, 10 and 11, 3m below the pile top. Strings of 16 (for large diameter piles) and 17 (for small diameter piles) FBG gauges were placed in 5mm square channels on the outside of the pile wall. They were bonded and coated with layers of cyanoacrylate, epoxy and hot melt adhesive glue. FBG sensors reflect light of a given wavelength, which is altered when the sensor is strained. For PICASO, a Micron Optics SM130 Dynamic Interrogator was used to record the wavelengths and to calculate the associated strain induced in the pile. The sampling frequency during driving was 5kHz.

P07 and P09 had four FBG strings while all other piles had two. Small diameter piles had one temperature gauge and 16 strain gauges, and large diameter piles had three temperature gauges and 13 strain gauges. Theoretically the temperature measurements can be used to calculate temperature insensitive strain measurements for the surrounding gauges, however this has not been applied to strain measurements in this paper due to reliability issues arising from the strain sensitivity of the temperature gauges (also encountered by Lovera, 2019 and Buckley et al., 2020a).

The layout of FBG, and where present PDA, gauges is illustrated in Figure 2.

4 MEASUREMENTS DURING PILE DRIVING

4.1 PDA measurements

PDA measurements of acceleration are integrated to give velocity and displacement of the pile with time, and measurements of strain ϵ are used to calculate force:

$$F = EA\epsilon \quad (1)$$

Where E is Young's modulus and A is cross-sectional area. Figure 5 shows the PDA pile force for an example blow near the end of driving for large diameter pile P09. Velocity, v , is multiplied by pile impedance:

$$Z = EA/c \quad (2)$$

Where c is the wave propagation speed. The resulting

F and Zv signals should be equal until prior to the first reflected wave reaching the instruments. The wave up force is half the difference between these signals, so is expected to be zero over this same period prior to reflection:

$$F_{up} = (F - Zv)/2 \quad (3)$$

In practice the peak force was generally measured to be 10-16% lower than the peak Zv . The measurement of acceleration was considered to be more reliable, so the force signal was multiplied by a factor of $(Zv)_{peak}/F_{peak}$. This resulted in wave up values prior to the first reflection of approximately zero as expected, with the exception of minor instrument noise.

4.2 Fibre optic measurements

Force is calculated from FBG and PDA strain measurements using Equation 1. As each pile has two or four FBG strings, the average is taken for all gauges at each level. For the purpose of signal matching, it was decided to re-zero the FBG strains at the start of each blow, as an accumulation of residual strain was observed in these measurements, but not the PDA measurements. The same behaviour was observed in stiff over-consolidated clay at Pentre (Randolph, 1993) and in chalk by Buckley et al. (2020a). The latter Authors attributed the response to locked in stresses in the steel and/or temperature effects in the steel.

The force calculated from above ground FBG strain gauges (gauge number 02) averaged across measurements from four strings for an example blow near the end of P09 driving is shown in Figure 4. This is compared with the force calculated from PDA measurements, located 7.85m from the FBG gauges, showing comparable values in peak force.

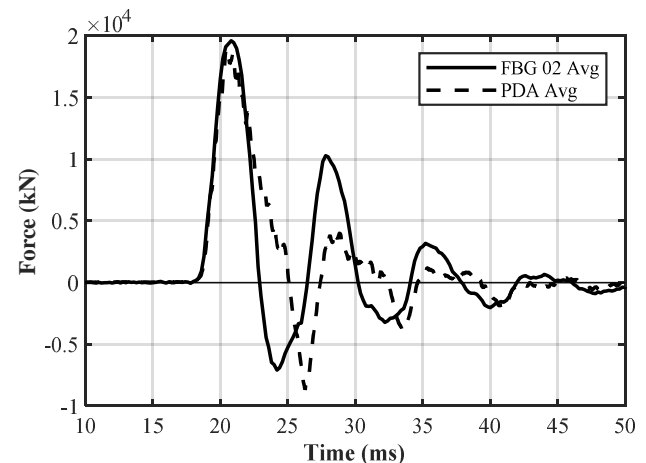


Fig. 4. Force measurements from PDA and above ground FBG strain gauges for P09 blow 914.

5 STRESS WAVE ANALYSIS

The research-oriented software program IMPACT (Randolph, 2008) was selected for stress wave analysis in the PICASO project. Following the conventional stress wave matching process, the known downward

travelling wave is applied to the pile top and an estimate of upward travelling wave is produced to compare to the measured signal. The estimated upward travelling wave is dependent on inputs of pile base and shaft resistance. The specific models in IMPACT use elasto-dynamic theory and are defined by Deeks and Randolph (1995) for base resistance, and Simons and Randolph (1985) for shaft resistance. The input parameters are iterated until the calculated upward wave matches well with the measured upward wave.

5.1 Input parameters

The shear modulus profile selected for stress wave analysis was taken as 10% of the G_{\max} profile shown in Figure 1. This reduction is required to account for soil nonlinearity, where secant modulus G is degraded from G_{\max} with increasing strain (Atkinson and Salfors, 1991; Mair, 1993). The extent of degradation was determined through iteration of the stress wave matching process with input G having a significant effect on the later portion of the wave and the displacement behaviour during a blow. Viscous parameters α and β were taken as 1 and 0.2 respectively, as recommended by Randolph (2008). The piles were assumed to remain unplugged throughout driving and soil resistance was assumed to act on the external area only.

5.2 Manual signal matching

Signal matching was performed using manual iterations with the software IMPACT for a number of individual blows. This paper will focus on four sample blows at different depths during the installation of large diameter pile P09. The selected blows and estimated corresponding embedment depths are 170 (3m), 379 (4.5m), 613 (5.99m) and 914 (7.46m). The total blow count for this pile was 922 and total embedment was 7.5m. The manual signal matching process assessed the match between calculated and measured wave up and pile head displacements. An example of these comparisons for blow 914 following completion of the manual iterative process is shown in Figure 5. The resulting profiles of mobilised shear stresses are shown in Figure 6. With minor exceptions, the mobilised shear stresses at any given soil horizon reduce as the pile is driven further, a phenomenon known as ‘friction fatigue’. Similar trends in over-consolidated stiff clays were observed from signal matching by Randolph (1993) and Buckley et al (2020c) at Tilbrook, onshore UK and the Wikinger offshore windfarm respectively.

Ultimate end bearing pressure at the base of the pile, q_b , was selected based on the local tip resistance measured by a CPT at the pile location. Through an iterative approach, $0.4q_t$ averaged over a range of 1.5m above and below the tip depth was found to produce a good match for P09. Across the other PICASO piles with PDA measurements, the ratio varied from 0.4 to $0.6q_t$. The shear stress profile was initially estimated from the CPT sleeve friction profile, and then varied iteratively.

Soil layers of 0.5m thickness were used for the development of the shear stress profile.

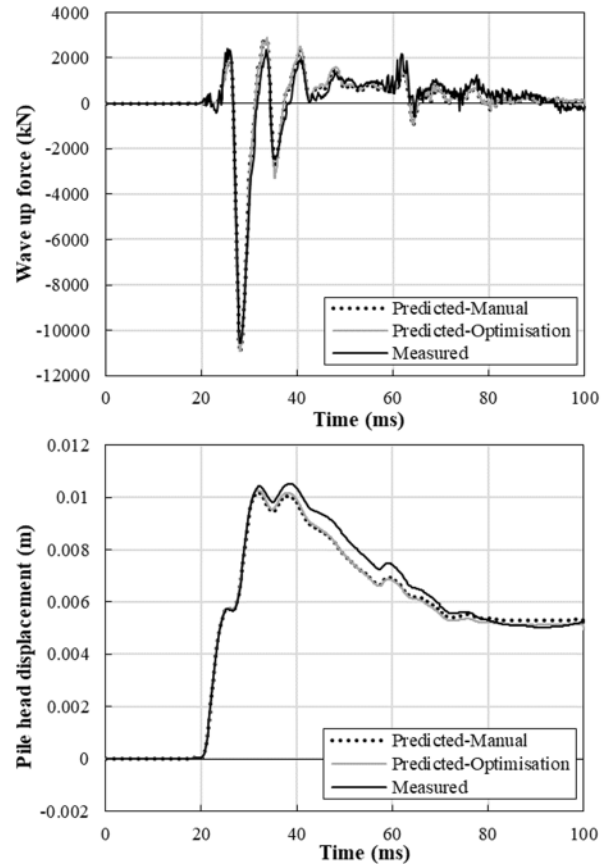


Fig. 5. Comparison of wave up force and displacement from manual and optimisation methods of signal matching with those measured by PDA for P09 blow 914.

5.3 Signal matching optimisation incorporating FBG measurements

A shortcoming of the signal matching approach is that the solution is non-unique, giving rise to subjectivity in determining the final parameter set (Fellenius, 1988). Buckley et al. (2020a) proposed a novel solution to reduce this issue, further constraining the signal matching process by also seeking to match the calculated force signal at nodes down the pile with FBG measurements. In addition, Buckley et al. (2020a) implemented this calculation into an automated optimisation procedure in Matlab, which iterates the shear stress profile to minimise the combined error between measured and calculated forces. The associated Matlab code has been further developed to apply to the PICASO pile and instrument configurations. It has also been extended to iterate the base resistance. The error in wave up force at the pile head compared to PDA measurements was weighted equally with the sum of the errors from nodal forces compared to FBG measurements as per equation 4 (Buckley et al., 2020a).

$$\zeta(\%) = 0.5 \times \frac{1}{n} \sum_{i=1}^n \frac{\zeta_f(i)}{F_{max}(i)} + 0.5 \times \left(\frac{\zeta_{f,up}}{F_{up,max}} \right) \quad (4)$$

Where n is the number of FBG strain gauges, $\zeta_f(i)$ is

the average root mean square error between measured and calculated force at strain gauge i , $F_{\max}(i)$ is the maximum measured force at strain gauge i , $\zeta_{f,\text{up}}$ is the average root mean square error between measured and calculated upward force at the pile head, and $F_{\text{up},\text{max}}$ is the maximum measured upward force at the pile head.

The four example blows have been analysed using: conventional signal matching only considering the PDA measurements; automated signal matching only considering the PDA measurements; and automated signal matching considering PDA and FBG measurements. Table 1 shows that the inclusion of FBG inputs leads to a small reduction in overall error, and with the exception of blow 170, higher values of mobilised base resistance. Both automated processes yield higher mobilised shaft resistance.

Table 1. Comparison of proportional error.

Blow no.	No optimisation PDA only		Optimisation PDA only		Optimisation PDA and FBG	
	Error, ζ (%)	Mobilised Res. (kN)	Error, ζ (%)	Mobilised Res. (kN)	Error, ζ (%)	Mobilised Res. (kN)
		Shaft Base		Shaft Base		Shaft Base
170	4.9	2356 221	4.8	2455 55	4.7	2593 91
379	5.0	2749 347	4.8	2967 87	4.6	2794 578
613	4.7	3586 381	4.4	4109 95	4.0	4148 694
914	4.5	4659 529	5.0	5513 132	4.1	5367 857

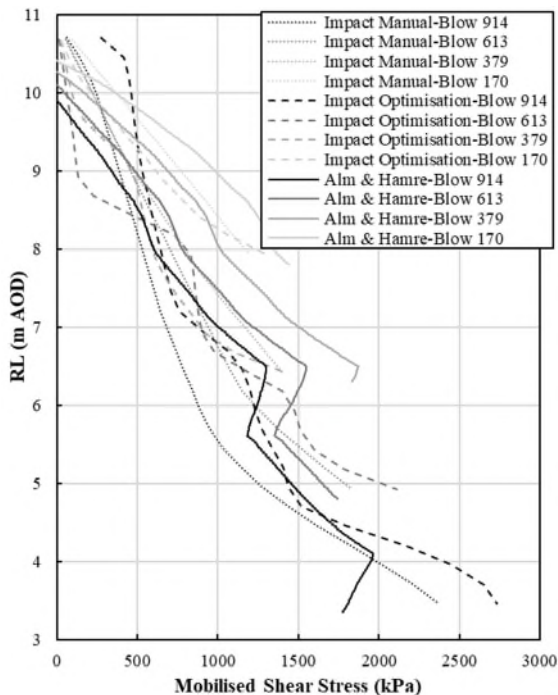


Fig. 6. Comparison of mobilised shaft resistance from manual and optimisation methods of signal matching with Alm and Hamre (2001) CPT correlation.

Figure 7 shows the measured and calculated force time histories for a selection of FBG strain gauges distributed over the embedded length for blow 914 using the results from the manual signal matching and optimisation including FBG inputs. It can be seen that

both the manual and optimised methods are consistently over predicting the maximum force compared to FBG measurements.

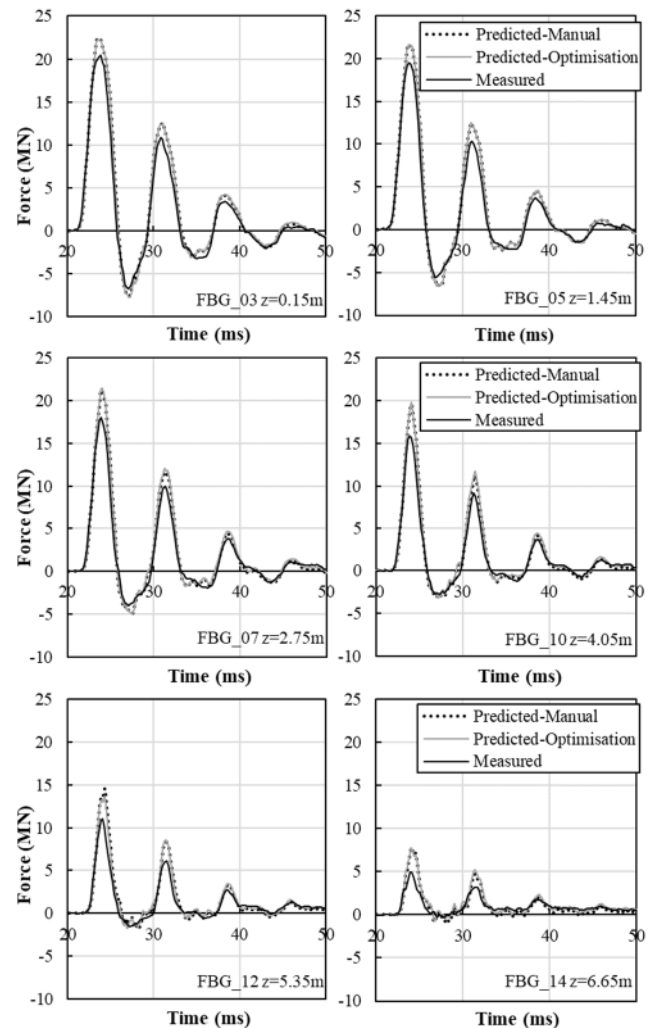


Fig. 7. Comparison of predicted force from manual and optimisation methods of signal matching with measured force at select FBG strain gauges from P09, blow 914.

6 SOIL RESISTANCE TO DRIVING

Accurate estimation of SRD is an important component in pile drivability predictions. The Alm and Hamre (2001) method, involving direct correlations with CPT data, is widely adopted by industry. From their own database, Alm and Hamre (2001) note that this method on average calculates slightly higher resistance than experienced during driving, which is conservative in terms of drivability analysis.

The mobilised shaft resistance calculated using this method has been compared to results from IMPACT calculations, with and without optimisation for the four example blows in Figure 6. For the shallower two blows, the Alm and Hamre (2002) method was conservative compared to both signal matching results, suggesting it may underestimate the friction fatigue for these blows. For the deeper two blows, the mobilised shear stresses are comparable between the three calculation methods,



with the Alm and Hamre (2002) profile appearing to be non-conservative in the 1m above pile tip in both cases.

With the exception of the deepest blow, Alm and Hamre (2002) provides maximum or near maximum values for base resistance. Blow 914 occurs at a depth where the pile toe is expected to be in a sandy silt layer based on the CPT profile at this location. The under-estimation of mobilised shear stress near the toe and base resistance for this blow suggests the Alm and Hamre (2002) method may not be conservative for sand layers.

7 CONCLUSIONS

This paper describes the extension of a novel signal matching procedure, proposed by Buckley et al. (2020a) to data from impact driving of 1.22m and 2.5m diameter tubular steel piles at the PICASO Cowden test site. Shear stress profiles and base resistance values with a small improvement in proportional error were successfully developed by applying this automated optimisation procedure, which supplements conventional PDA data with FBG strain measurements. The SRD calculated using this method was generally well predicted by the Alm and Hamre (2001) CPT correlation method. However the difference in mobilised shear stress and base resistance compared to those obtained through signal matching approaches, may offer additional insights into soil behaviour throughout driving, particularly in regard to the influence of sand or silt layers in an over-consolidated clay profile.

ACKNOWLEDGEMENTS

The authors acknowledge the support of Ørsted in funding the PICASO project. The authors also acknowledge Socotec as the principal contractor and Quinn Piling who installed the piles.

REFERENCES

- 1) Alm, T. and Hamre, L. (2001): Soil model for pile driveability predictions based on CPT interpretations, *Proceedings of the 15th International Conference on Soil Mechanics and Geotechnical Engineering*, Istanbul, Turkey, 2: 1297-1302.
- 2) Atkinson, J. H. and Salfors, G. (1991): Experimental determination of soil properties, *Proceedings of the 10th European Conference on Soil Mechanics and Foundation Engineering*, Florence, 915–956.
- 3) Boulton, G. S. and Paul, M. A. (1976): The influence of genetic processes on some geotechnical properties of glacial tills, *Quarterly Journal of Engineering Geology and Hydrogeology*, 9 (3): 159-194.
- 4) Buckley, R. M., McAdam, R. A., Byrne, B. W., Doherty, J. P., Jardine, R. J., Kontoe, S. and Randolph, M. F. (2020a): Optimization of impact pile driving using optical fiber Bragg-grating measurements, *Journal of Geotechnical and Geoenvironmental Engineering*, 146 (9).
- 5) Buckley, R. M., Byrne, B. W., Martin, S. C., McAdam, R. A., Sheil, B. B., Aghakouchak, A. and Lindeboom, R. (2020b): Large diameter pile testing for offshore wind applications with a focus on cyclic lateral loading and rate effects, *Proceedings of the 4th International Symposium on Frontiers in Offshore Geotechnics* (postponed), Texas, USA.
- 6) Buckley, R. M., R. J. Jardine, S. Kontoe, P. Barbosa and F. C. Schroeder (2020c): Full-scale observations of dynamic and static axial responses of offshore piles driven in chalk and tills, *Géotechnique* 70 (8): 657-681.
- 7) British Geological Survey (2015): Geology of Britain viewer, Available at: <<http://mapapps.bgs.ac.uk/geologyofbritain/home.html?>> [Accessed 2019].
- 8) Deeks, A. J., and Randolph, M. F. (1995): A simple model for inelastic footing response to transient loading, *International Journal of Numerical Methods in Geotechnical Engineering*, 19 (5): 307–329.
- 9) Fellenius B. H. (1988): Variation of CAPWAP results as a function of the operator, *Proceedings of the 3rd International Conference on the Application of Stress Wave Theory to Piles*, Ottawa, 814–825.
- 10) Lovera, A. (2019): Cyclic lateral design for offshore monopiles in weak rocks, Doctor of Philosophy, Université Paris-Est.
- 11) Mair, R. J. (1993): Unwin memorial lecture 1992. Developments in geotechnical engineering research: application to tunnels and deep excavation, *Proceedings of the Institute of Civil Engineers, Civil Engineering*, 97 (1): 27-41.
- 12) Powell, J. J. M. and Butcher, A. P. (2003): Characterisation of a glacial till at Cowden, Humberside, *Characterisation of Engineering Properties of Natural Soils*. T. S. Tan, K. K. Phoon, D. W. Hight and S. Leroueil. Lisse, The Netherlands, Swets & Zeitlinger B.V. 2: 983-1020.
- 13) Randolph, M. F. (1993): Analysis of stress-wave data from pile tests at Pentre and Tilbrook, *Recent Large-Scale Fully Instrumented Pile Tests in Clay*, Institution of Civil Engineers, London, UK.
- 14) Randolph, M. F. (2008): IMPACT—Dynamic analysis of pile driving, Crawley, Australia, Department of Civil and Environmental Engineering, University of Western Australia.
- 15) Simons H. A., and Randolph, M. F. (1985): A new approach to one dimensional pile driving analysis, *Proceedings of the International Conference on Numerical Methods in Geomechanics*, Cambridge, UK. 1457–1464.
- 16) Zdravković, L., Jardine, R. J., Taborda, D. M. G., Abadias, D., Burd, H. J., Byrne, B. W., Gavin, K. G., Houlsby, G. T., Igoe, D. J. P., Liu, T., Martin, C. M., McAdam, R. A., Muir Wood, A., Potts, D. M., Skov Gretlund, J. and Ushev, E. (2019): Ground characterisation for PISA pile testing and analysis, *Géotechnique*, 70 (11): 945-960.